Neutrophil Adhesive Contact Dependence on Impingement Force

C. M. Spillmann,* E. Lomakina,† and R. E. Waugh‡
*Department of Biochemistry and Biophysics, †Department of Pharmacology and Physiology, and ‡Department of Biomedical Engineering, University of Rochester, Rochester, New York

ABSTRACT Neutrophil capture and recruitment from the circulation requires the formation of specific receptor/ligand bonds under hydrodynamic forces. In the present study we examine bond formation between β_2-integrins on neutrophils and immobilized ICAM-1 while using micropipettes to control the force of contact between the cell and substrate. Magnesium was used to induce the high affinity conformation of the integrins, and bond formation was assessed by measuring the probability of adhesion during repeated contacts. Increasing the impingement force caused an increase in the contact area and led to a proportional increase in adhesion probability (from ~20 to 50%) over the range of forces tested (50–350 pN). In addition, different-sized beads were used to change the force per unit area in the contact zone (contact stress). We conclude that for a given contact stress, the rate of bond formation increases linearly with contact area, but that increasing contact stress results in higher intrinsic rates of bond formation.

INTRODUCTION

Neutrophil participation in host defense via the inflammatory response is initiated via a cascade of events involving rolling adhesion, firm adhesion, and eventual migration through the vascular wall. Neutrophils are carried through the circulatory system and into contact with the vascular wall where adhesion is initiated by specific receptor/ligand bonds. Initial capture and rolling interactions are primarily mediated by selectins and their ligands, whereas cell arrest is mediated by integrins located on the neutrophil surface (Lawrence and Springer, 1991). The importance of fluid shear forces for adhesion between neutrophils and endothelial-cell ligand-presenting surfaces was an important early finding in studies of leukocyte-endothelial interactions (Lawrence et al., 1990; Alon et al., 1996; Finger et al., 1996). Indeed, several studies have shown that cell arrest mediated by integrin bond formation does not generally occur unless the interaction is preceded by cell rolling (Lawrence and Springer, 1991; Rainger et al., 1997; Green et al., 2004). The mechanism for this facilitation of integrin bond formation by cell rolling is not thoroughly understood. It is thought that the rolling interaction (mediated by rapidly binding selectins) increases the time of interaction between regions of the cell and substrate allowing the slower integrin bonds to form (Riha et al., 2003). Cell rolling may also allow time for (or even initiate) signaling events to upregulate integrin affinity for endothelial ligand. In addition to increasing contact time, rolling interactions also have significant effects on the forces of interaction between cells and substrate. Therefore, a complete understanding of the facilitation of integrin bond formation by cell rolling requires more detailed information about how mechanical forces affect the dynamics of integrin bond formation.

On neutrophils, most integrins are members of the family of β_2-integrins, heterodimeric glycoproteins found on leukocytes and having in common the β_2 subunit (CD18). LFA-1 and Mac-1 are the principle members of this group. Both bind to the endothelial ligand intercellular adhesion molecule-1 (ICAM-1), a member of the immunoglobulin superfamily that is widely expressed on the vascular endothelium in response to stimulatory agents (Dustin et al., 1986). Conformational changes in LFA-1 and Mac-1 are necessary for ligand binding (Dransfield et al., 1992; Li et al., 1998). In vivo, these activating conformational changes are brought about by inside-out signaling, i.e., intracellular signaling cascades initiated by chemokines and other stimulatory mechanisms (see review by van Kooyk and Figdor, 2000). Similar conformational changes can be induced using divalent cations. Calcium stabilizes a low affinity form of LFA-1, inhibiting ICAM-1 binding, whereas manganese or magnesium in the presence of the calcium chelator EGTA promotes the LFA-1/ICAM-1 interaction (Dransfield et al., 1992; Tominaga et al., 1998). The effects of divalent ions on the affinity state of Mac-1 are different. Whereas calcium and/or magnesium are essential for integrin affinity changes induced by inflammatory mediators, manganese but not magnesium induces the active form of Mac-1 in the absence of cell activation (Altieri, 1991; Diamond and Springer, 1993). Even though magnesium appears to act only on LFA-1, we have demonstrated previously that Mg^{2+} increases the likelihood of integrin-mediated homotypic adhesion between neutrophils (Spillmann et al., 2002) and enables adhesion between neutrophils and immobilized ICAM-1 (Lomakina

Submitted July 20, 2003, and accepted for publication September 1, 2004.

M. Spillmann and E. Lomakina contributed equally to this work.

Address reprint requests to Richard E. Waugh, Dept. of Biomedical Engineering, University of Rochester, Medical Center Box 639, 601 Elmwood Ave., Rochester, NY 14642. Tel.: 585-275-3768; Fax: 585-273-4746; E-mail: waugh@seas.rochester.edu.

0006-3495/04/12/4237/09 $2.00

doi: 10.1529/biophysj.103.031773

and Waugh, 2004). Thus, suspension of cells in buffers containing Mg^{2+} and EGTA is an effective way to promote integrin-mediated neutrophil adhesion to ICAM-1 without general activation of the cell.

Prior studies addressing the role of mechanical force and leukocyte deformation during adhesion have focused on adhesion and cell deformation under flow (Firrell and Lipowsky, 1989; Dong et al., 1999; Lei et al., 1999; Dong and Lei, 2000). Neutrophil attachment to a ligand-coated substrate under fluid shear results in cell deformation and a corresponding increase in the contact area between the two surfaces. In these prior studies, investigators have argued that this should facilitate cell recruitment by increasing the area over which adhesive bonds can form and by prolonging the duration of contact, allowing more time for bonds to form. In addition, increasing the size of the contact area between the cell and substrate alters the mechanical forces acting at the adhesive interface and reducing the magnitude of detachment forces at the trailing edge of the cell. An important aspect of the adhesion process that has not been considered in prior studies is the effect that impingement forces between the cell and the substrate may have on the rate of bond formation.

As an approach for assessing the effect of mechanical force on adhesive bonds in the contact zone, flow channel studies have a number of intrinsic disadvantages. The contact area and the duration of contact between the two surfaces are not easily resolved experimentally and vary in a complex way with the magnitude of shear forces on the cells and the formation and breakage of bonds in the contact zone. These difficulties have forced investigators to make approximations and assumptions about the magnitude and distribution of bond forces in the contact zone to extract estimates of coefficients of bond breakage in the contact zone (Chang et al., 2000; Greenberg et al., 2000; Bhatia et al., 2003). In the present study we overcome many of these difficulties by using a micropipette technique that has been applied to study adhesion and two-dimensional bonding kinetics (Spillmann et al., 2002; Lomakina and Waugh, 2004). It provides a direct measure of the adhesion probability while controlling the force, duration, and area of contact between the two interacting surfaces (Chesla et al., 1998; Levin et al., 2001; Spillmann et al., 2002). Using this approach, we have examined the effect of impingement force on bond formation between neutrophils and immobilized ICAM-1. In a companion report we present a mechanical analysis of the increase in contact area with force, and we predict that the contact stress (force per unit area of contact) depends not on the force, but on the curvature of the contacting surfaces. In the present study we find that the rate of bond formation at a given contact stress increases in direct proportion to the contact area, but that increasing contact stress by increasing the curvature of the contacting bead causes an increase in the intrinsic rate of bond formation.

METHODS

Cell preparation

Neutrophils from a drop of whole blood obtained via a finger stick were diluted into Hank's Balanced Salt Solution without Ca^{2+} or Mg^{2+}, 10 mM HEPES, and 4% heat-inactivated fetal bovine serum (FBS, Hyclone, Logan, UT), pH 7.4, 290 mOsm. The suspending solution for measuring cell adhesion contained 10 mM HEPES, 145 mM NaCl, 5 mM KCl, 2 mg/ml glucose, 4% FBS, and either 5 mM $MgCl_2$ plus 0.5 mM EGTA, or 1.5 mM Ca^{2+} (pH 7.4, 290 mOsm).

Bead preparation

Two types of beads were used in this study. Most experiments were performed with tosyl-activated, paramagnetic Dynabeads (Dynal, Lake Success, NY). The manufacturer supplies these beads in two nominal sizes: 2.8 μm and 4.5 μm. The beads were coated with soluble recombinant forms of two members of the IgG superfamily: either ICAM-1 (R&D Systems, Minneapolis, MN) or neural cell adhesion molecule (NCAM, Chemicon International, Temecula, CA). The molecules were randomly and covalently linked via active tosyl groups to the bead surface. Beads (10^7) were washed twice in 1.0 ml of 0.1 M phosphate buffer (pH = 7.4) then incubated in 1.0 ml of phosphate buffer plus 1.2 μg of ICAM-1 or 5 μg of NCAM (4.5-μm beads), or 2 μg of ICAM-1 (2.8-μm beads) at room temperature overnight. Unreacted tosyl groups were blocked by a 30-min incubation with 8 mM ethanolamine and then washed twice with 1% bovine serum albumin (BSA, Calbiochem-Novabiochem, La Jolla, CA) in phosphate-buffered saline (PBS, BioWhittaker, Walkersville, MD) and stored in 0.1% BSA in PBS at 4°C.

For some experiments carboxylated beads (Polysciences, Warrington, PA) were used to obtain a wider range of diameters (3.0 μm and 10.0 μm). The beads were first coated with protein-G and then with soluble recombinant forms of human ICAM-1/Fc chimera (R&D Systems) and human NCAM-L1/Fc chimera (R&D Systems). First, protein-G was covalently linked to carboxylated bead surface. Beads were washed twice in 0.1 M carbonate buffer and allowed to mix in 2% carbodiimide solution for 3–4 h. Then beads were washed in 0.02 M phosphate buffer and incubated in 1 ml of 0.2 M borate buffer plus 320 μg of protein-G overnight at room temperature. After unreacted sites were blocked by a 30-min incubation with 4 mM ethanolamine, the beads were resuspended in 1% BSA and incubated for 30 min at room temperature to block any remaining nonspecific protein binding sites.

After beads were coated with protein-G, recombinant forms of ICAM-1/Fc chimera and NCAM-1/Fc chimera were covalently linked to the surface of the beads. For that, 20 μl of the protein-G-coated beads were sonicated for 5 min in 1 ml of BlockAid solution (Molecular Probes, Eugene, OR) to reduce nonspecific binding. Then either 5 μg of ICAM-1/Fc chimera (3-μm beads) or the mixture of 4.5 μg of ICAM-1/Fc and 0.5 μg of NCAM-L1/FC chimeras (10-μm beads) were added to the bead suspension and incubated for 40 min at room temperature on a rotating platform. The beads were washed twice in 0.2 M triethanolamine (Sigma, St. Louis, MO), pH 8.2, and resuspended in 0.5 ml of 0.2 M triethanolamine, containing 20 mM dimethyl pimelimidate (Sigma) to cross-link the chimera to the protein-G. After a 30-min incubation at room temperature, the reaction was stopped by adding 0.5 ml of 50 mM Tris (Sigma), pH = 7.5 with rotational mixing for 15 min. The cross-linked beads were washed twice in 0.1% BSA, 0.05% Tween 20 (Fisher Scientific, Fair Lawn, NJ), and 0.1% sodium azide in PBS and stored in the same washing buffer at 4°C.

The density of ICAM-1 on the beads was measured by flow cytometry (Lomakina and Waugh, 2004). Ligand-coated beads were incubated with FITC-conjugated mouse-anti-human ICAM-1 (clone 15.2, Ancell, Bayport, MN) or an isotype-matched control antibody at 4°C overnight. The antibody 15.2 recognizes the distal domain (D1) of ICAM-1 and inhibits binding to LFA-1 (Staunton et al., 1990). Fluorescence intensity was correlated to the

number of bound antibodies on the coated beads using Quantum Simply Cellular Beads (Flow Cytometry Standards, Fishers, IN) as a calibration standard. Beads coated with NCAM served as nonspecific controls for adhesion tests, and the presence of NCAM on the surface was confirmed by incubation with a primary antibody followed by FITC-labeled secondary antibody.

Adhesion tests

The micromanipulation procedure is adapted from one introduced first by Shao and Hochmuth (1996) and Shao et al. (1998) and previously used in our laboratory (Spillmann et al., 2002). A detailed description is provided in a companion report (Lomakina et al., 2004). Diluted blood was placed in a chamber on the stage of an inverted light microscope (Diaphot, Nikon, Garden City, NY). Passive spherical neutrophils were selected from diluted blood suspension on the basis of their multilobular nuclei. (To validate our selection method, cells were selected as if for mechanical measurement, then transferred with a micropipette onto a cover glass and stained. More than 85% of the selected cells were neutrophils as assessed by Wright's stain.)

After selection, neutrophils were transferred into a second chamber using a large micropipette (9–10 μm inside diameter, I.D.) and then allowed to equilibrate for at least 20 min with the suspending solution (or 40 min if an antibody was present). The chamber was open on opposite sides to accommodate opposing micropipettes and contained a dilute suspension of the ICAM-coated beads. Pipettes were filled with Hank's Balanced Salt Solution without Ca^{2+} or Mg^{2+}, and positioned inside the touch chamber. Before measurement, a negative pressure was applied for 15 min to draw in protein solution and reduce unwanted neutrophil adhesion to the pipette lumen. A neutrophil was aspirated into the large pipette, and a small pipette ($\sim$2 μm I.D.) was used to position a bead inside the larger pipette (Fig. 1). After the zero pressure was set, a touch sequence was initiated by creating a positive pressure to push the cell into contact with the bead. For each cell bead pair four different impingement pressures in the range of $\sim$1.0 to $\sim$6.0 pN/μm^2 (0.1–0.6 mm H_2O) were tested. The equilibrium pressure in the translation pipette was periodically checked, and typical deviations were $<$0.5 pN/μm^2. (In addition, the free velocity of the cell in the pipette was measured, a posteriori, to ensure the pressure remained steady for repeated tests.) After $\sim$2 s of contact, the neutrophil was drawn away from the bead by closing a solenoid valve to apply a suction of $\sim$2.0 pN/μm^2. Contacts were repeated 25 times at each of four different impingement pressures for each cell/bead pair, and three or four cells were tested on a given day of experiment. All measurements were performed at room temperature (22°C). Adhesion tests were recorded on videotape with a time stamp and the withdrawal and impingement pressure overlaid on the image. Distances were calibrated using a stage micrometer.

Several different control conditions were tested. In one, Mg^{2+} and EGTA were replaced with 1.5 mM Ca^{2+}. In another, ICAM-coated beads were replaced with NCAM-coated beads. Third, the β_2-integrin blocking antibody IB4 (mouse anti-human CD18, 10 μg/ml, Ancell) was introduced into the suspending medium in which the adhesion measurements were performed. To test for nonspecific effects of antibody binding to the cells, an isotype antibody against a transmembrane tyrosine phosphatase found on neutrophils (anti-CD45, Ancell) was added to the suspending solution (10 μg/ml).

Video recordings of the experiments were analyzed to determine what fraction of the contacts resulted in adhesion between the cell and the bead. An adhesive contact was signified by either a small deformation of the neutrophil surface during separation or (in some rare cases) the formation of a thin tube of membrane, a tether, upon withdrawal from the contact zone. The final probability of forming an adhesive contact between a particular neutrophil and bead was calculated as the number of adhesive contacts divided by the total number of touches. The total averaged adhesion probability for β_2-integrin/ICAM-1 binding was corrected to account for nonspecific adhesion according to Chesla et al. (1998),

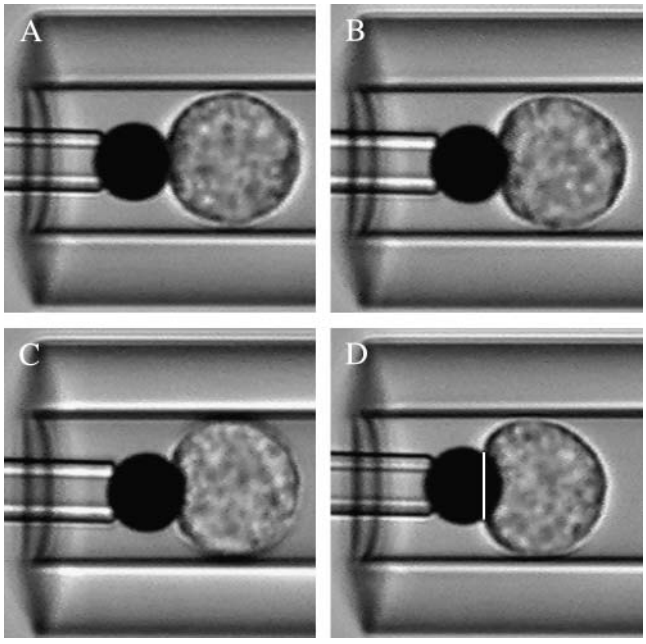

FIGURE 1 This series of video micrographs shows a neutrophil in contact with an ICAM-1-coated bead (4.5-μm diameter) at four different impingement pressures. Beads were held approximately one neutrophil diameter within the translation pipette to maintain alignment of the cell and bead. The impingement forces for the different images (from *A–D*) were $\sim$70 pN, $\sim$140 pN, $\sim$210 pN, and $\sim$280 pN. The contact area between the two surfaces was determined from measurement of the contact length L_{con}, the distance between the two points in the cross-section where the bead and cell intersect. (See vertical line in *D*.)

$$P_{adh} = \frac{P_t - P_n}{1 - P_n}, \tag{1}$$

where P_t is the total adhesion, P_n accounts for nonspecific adhesion, and P_{adh} is the adhesion probability specific to β_2-integrin and ICAM-1 binding.

In addition to the adhesion probability, the contact area and the force of impingement were determined. The contact area was determined by measuring the contact length (two times the radius of the contact zone), $L_{con} = 2R_{con}$, from video recordings (Fig. 1). The macroscopic contact area is given by

$$A_{mac} = 2\pi R_b\left(R_b - \sqrt{R_b^2 - R_{con}^2}\right), \tag{2}$$

where R_b is the bead radius. The force (at equilibrium) was calculated accounting for the fluid leak between the cell and pipette wall according to the approach developed by Shao and Hochmuth (1996),

$$F = \pi R_p^2 \Delta p_{im}/C_1, \tag{3}$$

where Δp_{im} is the impingement pressure. The constant C_1 is

$$C_1 = 1 + \frac{4\varepsilon}{3} + \frac{16(L_{eq} - D_c)}{9\pi R_p}\left(\varepsilon^{5/2}\sqrt{2} - \frac{4\varepsilon^3}{\pi}\right), \tag{4}$$

where D_c is the diameter of the cell, L_{eq} is the equivalent tube length of the pipette, and $\varepsilon = (R_p - R_c)/R_c$ is the dimensionless film thickness between the

cell and the wall of the pipette. The quantities L_{eq} and ε are obtained from measurements of the free velocity of the cell in the pipette as described in the companion report (Lomakina et al., 2004).

Other quantities

The adhesion probability is related to the average number of bonds formed in the contact zone, $\langle n \rangle$ (Chesla et al., 1998),

$$\langle n \rangle = -\ln(1 - P_{adh}). \quad (5)$$

This expression accounts for the occurrence of multiple bonds and assumes that bond formation follows Poisson statistics (Capo et al., 1982). Two groups have shown that the expected number of bonds can be written in terms of a kinetic expression of the form (Chesla et al., 1998; Lomakina and Waugh, 2004)

$$\langle n \rangle = A_c \rho_c \rho_b K_a (1 - e^{-k_r t}), \quad (6)$$

where A_c is the area of contact between the two surfaces, ρ_c and ρ_b are the density of receptors (on the cell surface) and ligands (on the bead surface) in the contact area, K_a is the equilibrium association constant, k_r is the reverse rate constant, and t is the interaction time between the two surfaces. Eq. 6 indicates that for a given set of conditions, the expected number of bonds should increase in direct proportion to the contact area. It is important to recognize that K_a and k_r are effective kinetic constants that may be affected by a variety of extrinsic factors, such as surface topography and the distribution and mobility of adhesion receptors in the surface. (Note: in the present report we do not distinguish between the area of contact A_c in Eq. 6, and the macroscopic area of contact A_{mac} given in Eq. 2. In fact, the actual area within the contact zone where bonds can form is some (unknown) fraction of the macroscopic contact area because of the irregularity of the cell surface. In our treatment, we lump the ratio of the true contact area to the macroscopic contact area A_c/A_{mac} into the effective equilibrium coefficient K_a.) The dependence of the expected bond number on contact stress is a particular focus of the present study. To evaluate this, the contact stress can be calculated through the relationship

$$\sigma = 2T_{cort}\left(\frac{1}{R_b} + \frac{1}{R_c}\right), \quad (7)$$

where R_c is the cell radius, and T_{cort} is its cortical tension.

RESULTS

Force dependence of adhesion

In the first series of experiments, 12 cell-bead pairs were tested at each of four different impingement pressures. In the presence of Mg^{2+} and EGTA, all cells showed elevated adhesion probability relative to controls. The number of sites on the beads used in this experimental series was determined by flow cytometry to be ~290 sites/μm^2, and the contact duration was ~2.0 s. Significant variability in adhesion probability was observed among different cells, but for each cell the adhesion probability increased with increasing force. Three examples are shown in Fig. 2 *A*. To avoid biasing the data from a possible history-dependence of cell adhesion, the order of application of the impingement pressures was 1.5, 6.0, 3.0, then 4.5 pN/μm^2. In Fig. 2 *B*, the data are grouped according to the impingement pressure, and the horizontal error bars represent the standard deviation of the calculated force at that pressure for the 12 cells. The nearly linear relationship between the mean adhesion probability and the mean force is an accurate reflection of the fact that this is the behavior typically observed for individual cells. The large standard deviation reflects the variability from one cell to another. The range of control values is shown in expanded scale in Fig. 2 *C*. Introduction of the β_2-blocking antibody IB4, replacement of ICAM-1 with NCAM on the bead surface, or substitution of calcium for Mg^{2+}/EGTA in the suspending buffer all caused similar reductions in adhesion probability. Use of a non-β_2-blocking antibody (anti-CD45, a tyrosine phosphatase found on the neutrophil surface) in the presence of Mg^{2+}/EGTA caused a slight (not statistically significant) increase in cell adhesion.

From theoretical expectations based on first-order kinetics, Eq. 6, the formation of adhesive bonds should increase linearly with the area of contact between the neutrophil and bead. The fitted line to the control data (Fig. 2 *C*) was used to correct the data in Fig. 2 *B* for nonspecific adhesion according to Eq. 1. The resulting specific adhesion probabilities were then reexpressed as the expected bond number $\langle n \rangle$ according to Eq. 5. This quantity $\langle n \rangle$ is shown in Fig. 3 *A* as a function of the contact area for all 12 neutrophil-bead pairs. For individual pairs, the expected increase in bond formation with impingement force was consistently observed, but there was considerable variability in the slope of this dependence from cell to cell. A linear regression to the data for each cell is included as a guide for grouping data from individual cells. In Fig. 3 *B* the data are grouped according to impingement pressure, and the error bars represent the standard deviation of the measured contact area and the calculated bond number for the 12 cell-bead pairs. A weighted (1/variance) linear regression to the data is shown as the solid line, and the dashed line corresponds to a weighted regression to the three highest pressure points, fixed at the origin. Despite the variability from cell to cell, averaged values for the population show a remarkably linear relationship between the expected bond number, $\langle n \rangle$, and contact area (Fig. 3 *B*).

Dependence of adhesion on contact stress

An important unresolved question is the extent to which cell adhesion rates might be affected by mechanical deformation of the cell surface. Compression of the microvilli on the cell surface could increase cell adhesion by at least two mechanisms. First, it would increase the percentage of membrane area in the contact zone that comes into intimate contact with the bead surface. Second, if molecules are distributed nonuniformly on the cell surface (particularly if the relevant molecules are excluded from the tips of microvilli), it could affect the concentration of molecules capable of binding to the substrate. The magnitude of microvillus

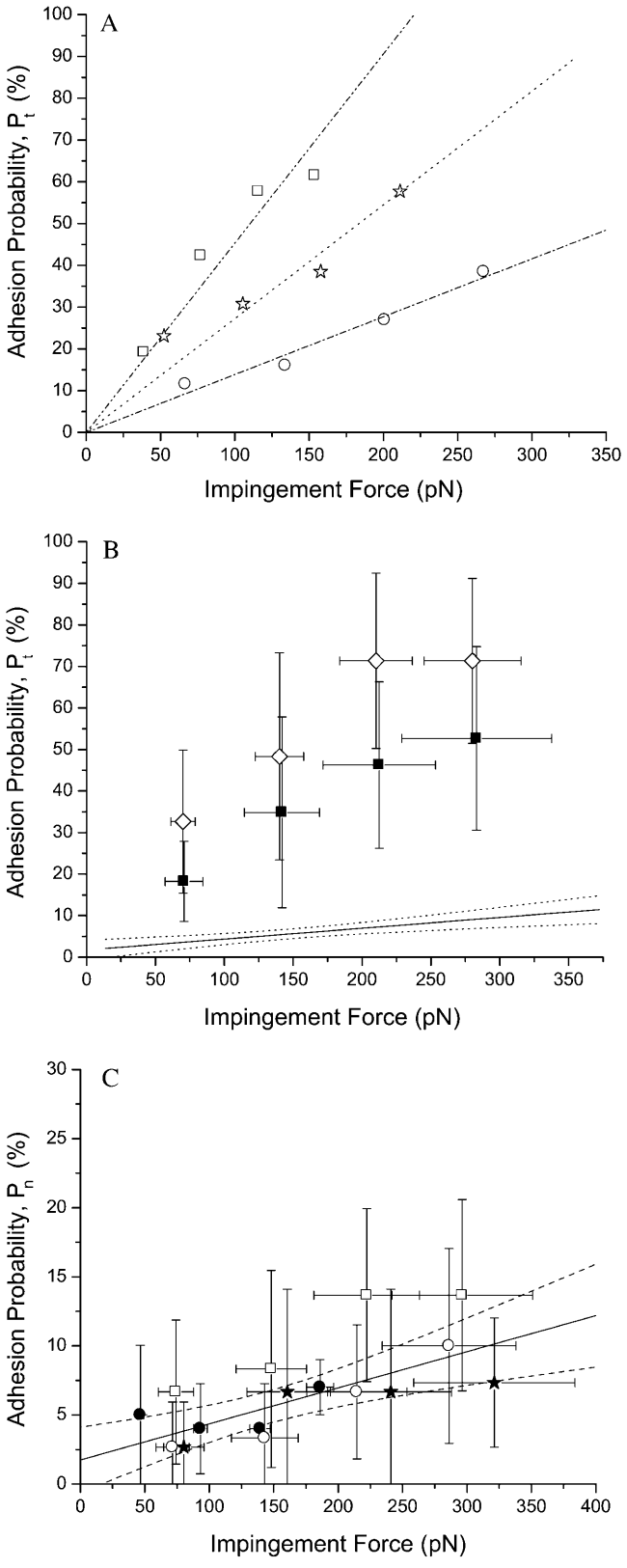

FIGURE 2 Adhesion probability of neutrophils binding to ICAM-1 beads as a function of the impingement force. (*A*) Increase in the adhesion probability with force in the presence of 5 mM Mg^{2+} for three individual cell-bead pairs. Different symbols correspond to different cells. Pearson's *r*-coefficients for the fits were 0.96, 0.97, and 0.98. (*B*) Mean adhesion probability for 12 cell-bead pairs as a function of impingement force. Data are grouped by impingement pressure and error bars represent the standard deviation of the values obtained for the 12 cells tested (■). Addition of an IgG control antibody caused a statistically insignificant increase in the adhesion probability (◇). Nonspecific adhesion probability under control conditions (see *C*) is indicated by the solid line with 95% confidence intervals shown by the dotted lines. (*C*) Several conditions were used to determine the level of nonspecific binding and demonstrate specificity of β_2-integrin binding to the ICAM-1 beads. The conditions were 5.0 mM Mg^{2+} plus 10 μg/mL of the β_2-blocking antibody IB4 (□), 5.0 mM Mg^{2+} with NCAM-coated beads (★), 1.5 mM Ca^{2+} (●), and 1.5 mM Ca^{2+} plus 10 μg/mL IB4 (○). Data is reported as the mean ± SD and grouped by the impingement pressure. The lines indicate a variance-weighted linear regression to the mean values, and dashed lines show the 95% confidence interval of the fit. Note the different vertical scale in *C*.

compression should depend on the force supported by individual microvilli, and this should in turn depend on the contact stress, or force per unit macroscopic area of contact. Mechanical analysis of the contact between the neutrophil and bead reveals that the equilibrium contact stress should be independent of the total force, but that it should increase with increasing curvature of the substrate. (See companion report and Eq. 7.)

To test for contact stress effects, a series of experiments was performed with different-sized beads. Four different bead preparations were tested, two with ICAM-1 bound by tosyl activation (2.8- and 4.5-μm diameter) and two with ICAM-1 chimera bound via protein-G (3.0- and 10-μm diameter); see Methods. As measured by flow cytometry, the number of ICAM-1 binding sites on these beads was found to be ~140 sites/μm^2 for 2.8-μm beads, ~290 sites/$\mu m^2$for 4.5-μm beads, ~640 sites/μm^2 for 3.0-μm beads, and ~800 sites/μm^2 for 10-μm beads. We then compared the intensive bond formation rate, that is, $\langle n \rangle$ normalized for contact area and surface density of ICAM-1. The results are shown in Fig. 4. For each case 7–12 cell bead pairs were tested. The impingement force was adjusted such that the mean contact areas were similar for each of the different groups (~6.0 μm^2). The contact stress was calculated based on a mean value of the cortical tension of 20 pN/μm. For both types of beads tested, a significant increase in the intrinsic rate of bond formation was observed with increasing contact stress. For the protein-G-conjugated beads, a doubling of the contact stress resulted in a twofold increase in bond formation, and for the tosyl-activated beads, a 30% increase in stress resulted in a 35% increase in bond formation.

DISCUSSION

Determinants of bond formation between cells and a substrate are more complex than the formation of bonds in solution. In addition to the intrinsic affinity between ligands and receptors, adhesive bond formation is affected by a number of extrinsic factors, including the distribution and mobility of molecules on the two surfaces (Bell, 1978) and the

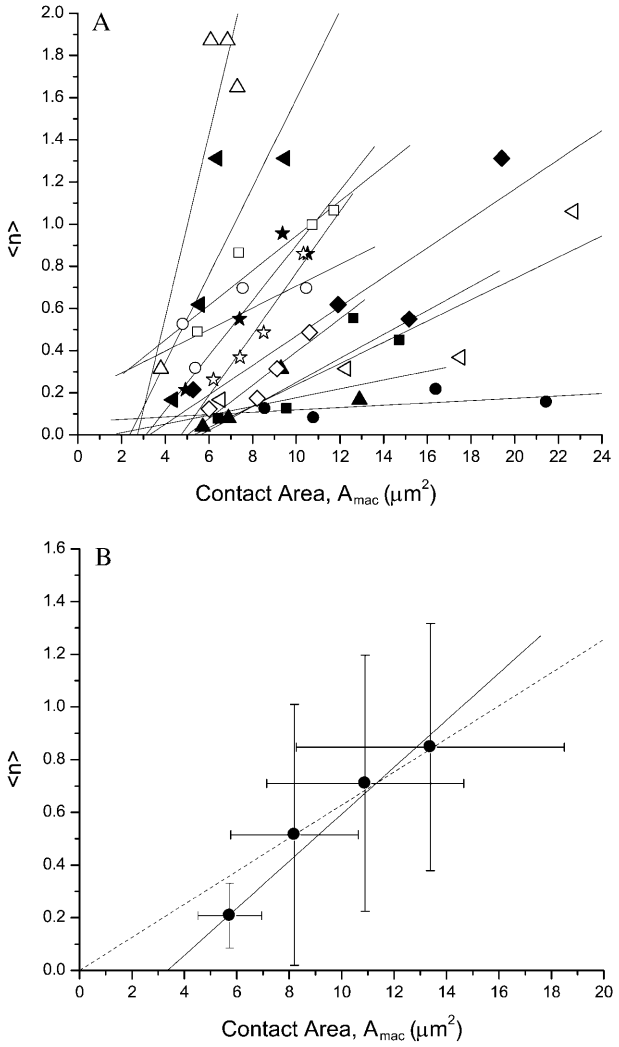

FIGURE 3 Relationship between the expected bond number, $\langle n \rangle$, and contact area. The values of $\langle n \rangle$ were corrected to account for nonspecific adhesion. (*A*) Data is shown for all cells tested, each cell represented by a different symbol. Solid lines show the linear regressions to each cell as a guide for identifying different points from the same cell. For most of the cells tested, the Pearson's *r*-value for the fits ranged from 0.8 to 0.98, but two cells have values of 0.54 and 0.58 and one cell had a value of 0.73. (*B*) The same data grouped according to impingement pressure. Error bars represent standard deviations of the distribution of force (*horizontal bars*) and expected bond number (*vertical bars*). The solid line is a linear regression to the four mean values weighted by the inverse of the variance (Pearson's $r = 0.99$). The dashed line is a linear regression to the data at the highest three pressures, fixed at the origin (Pearson's $r = 1.0$).

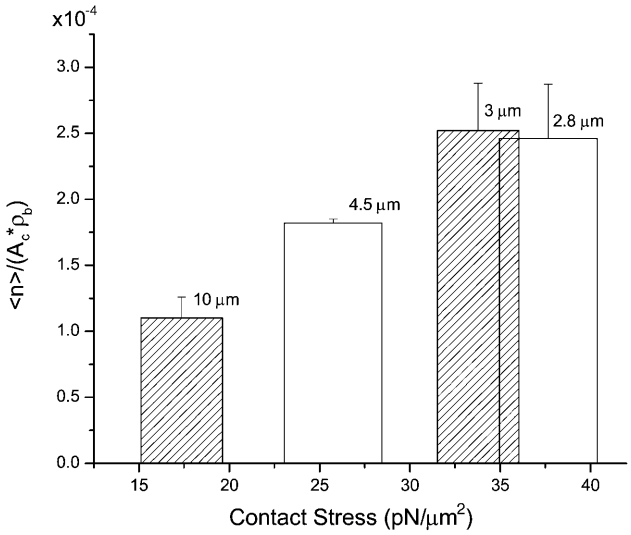

FIGURE 4 Changes in the intrinsic rate of bond formation with increasing contact stress. Open bars indicate results obtained with tosyl-activated beads and shaded bars indicate results obtained with protein-G-conjugated beads. Site densities on the beads were ~140 sites/μm^2 for 2.8-μm beads, ~290 sites/μm^2 for 4.5-μm beads, ~640 sites/μm^2 for 3-μm beads, and ~800 sites/μm^2 for 10-μm beads. Contact areas were in the range of 6.0 μm^2 for all measurements. The expected bond number was calculated according to Eq. 5. Contact stress was calculated according to Eq. 7. Increasing contact stress results in a significant increase in the expected bond number.

microtopography of the surface itself (Williams et al., 2001). The present findings demonstrate important effects of mechanical force on the specific case of integrin bond formation between neutrophils and immobilized ICAM-1. In the first place, force affects adhesion by the simple, direct mechanism of increasing the contact area between the cell and substrate, causing an increase in adhesion probability that is in direct proportion to the contact area. This is analogous to increasing the reaction volume for a conventional chemical reaction. Naively, one might expect that increasing force would also increase the compressive stress between the surfaces in the contact zone. Yet in our companion report, we demonstrate that the mechanical characterization of the cell as a liquid drop leads to the prediction that the contact stress should not depend on force, but should depend on the curvature of the contacting surfaces. Thus, the linear increase in bond formation rate with contact area is completely consistent with both kinetic expectations (Eq. 6) and the mechanical analysis predicting that any higher order effects due to changing contact stress should not be observed. On the other hand, when the contact stress is increased (by increasing the curvature of the contacting surface), an increase in the intensive rate of bond formation is observed. This is consistent with the expectation that compression of the microvilli on the cell surface should enhance cell adhesion.

It seems likely that the increase in adhesion with increasing contact stress is due to a mechanically induced change in the microtopography of the cell surface. Williams et al. (2001) demonstrated that cell membrane topography can have a substantial influence on the effective association rate between a receptor and ligand. For different cell surfaces (one smooth, one covered with microvilli) they report a 50-fold difference in the binding affinity for the same molecular pair (Williams et al., 2001). Shao et al. (1998) have estimated the compliance of microvilli subjected to pulling forces and estimate a spring constant of ~40 pN/μm. For contact stresses of 26–36 pN/μm^2, and assuming ~5 microvilli/μm^2

(Shao et al., 1998), the force supported by each microvillus is 5.0–7.0 pN. If the spring constant in extension is the same as that in compression, this would lead to a decrease in the microvillus length of 125–175 nm, a substantial fraction of the total microvillus length (100–300 nm). These calculations indicate that the effect on surface topography of the contact stresses applied in our study could be substantial.

A direct implication of these findings is that the surface topography of the bead surface could also have a substantial influence on adhesion rates. We have anecdotal evidence that this is indeed the case. Our original experimental design included three different-sized protein-G coupled beads, but the 6.0-μm diameter beads behaved very differently from the 3.0- and 10.0-μm beads. They showed uncharacteristically high levels of ICAM-1 uptake during the coating process, and even when the coating conditions were adjusted to obtain similar surface concentrations of ICAM-1, the intrinsic bond formation rates were substantially higher than expected for these beads. Examination of the bead surfaces by scanning electron microscopy revealed that the 6.0-μm beads had highly irregular surfaces with many protrusions and hole-like structures. In contrast, both the 3.0-μm and the 10.0-μm beads had smooth surfaces with only minor irregularities.

In addition to changing the percentage of membrane area in contact with the substrate within the contact zone, it is also possible that deformation of the cell surface could alter the number and type of molecules in contact with the bead. Several studies have indicated that adhesion molecules are nonuniformly distributed over the neutrophil surface (Erlandsen et al., 1993). If integrins are sequestered away from the tips of microvilli, as ultrastructural evidence indicates, then increasing the proportion of membrane in contact with the bead could result in a disproportionate increase in the concentration of integrin molecules capable of reacting with the ICAM-1 on the bead surface. This possibility is difficult to evaluate given existing information. Ultrastructural studies examining the distribution of adhesion molecules on leukocyte surfaces have used labels against Mac-1 (Erlandsen et al., 1993) or CD-18 (Fernandez-Segura et al., 1996) and have not examined the distribution of LFA-1 specifically. This is critical for our adhesion studies conducted in the presence of Mg^{2+} because under these conditions it is most likely that LFA-1 is the primary form mediating the adhesion to ICAM-1. That LFA-1 is the active form is supported by experiments conducted previously in our laboratory using blocking antibodies (Lomakina and Waugh, 2004) and is consistent with early reports that there is a significant increase in LFA-1 binding to ICAM-1 in Mg^{2+} (Dransfield et al., 1992), but that Mac-1 affinity is only slightly increased (Diamond and Springer, 1993). Thus, conclusions about whether the type and concentration of integrins in the contact zone may change with increasing contact stress must await further study.

Individually, and in aggregate, the bond formation rate of neutrophils appears to increase linearly with contact area, and the intrinsic rate of bond formation increases with contact stress. However, the adhesive potential can differ significantly from cell to cell. The reason for this heterogeneity is not apparent. One possibility is that it reflects differences in cell age or in the experience of the cells before removal from the circulation. For all cells tested, there were no visible signs of cell activation; that is, we observed no changes in morphology such as cell ruffling or the formation of pseudopodia. In a previous study, we used flow cytometry to show that magnesium and calcium solutions do not affect the expression of β_2-integrin or selectin molecules on the neutrophil surface, a further indication that, under the conditions of our study, cells remain in an essentially passive state (Spillmann et al., 2002).

Our present findings suggest that increasing impingement forces at the leading edge of the cell may be an important mechanism involved in the transition from rolling to firm, integrin-mediated attachments. This idea is supported by approximate calculations showing that the magnitudes of the contact stresses in our study are comparable to those that a cell is likely to experience in vivo. Similar calculations have been performed by others, but with a focus on the magnitude of peeling forces at the trailing edge of the cell (Alon et al., 1995; Dong et al., 1999). We summarize an approach here to estimate the impingement stress in the contact zone. Fluid forces acting on the cell and tangential force resultants on bonds at the interface create a torque on the cell that must be balanced by a force-couple created by peeling forces at the trailing edge of the cell and impingement stress in the contact region (Fig. 5). We assume that the contact area is circular, with a radius between 2.0 and 4.0 μm (Firrell and Lipowsky, 1989). We apply a hydrodynamic solution (Goldman et al.,

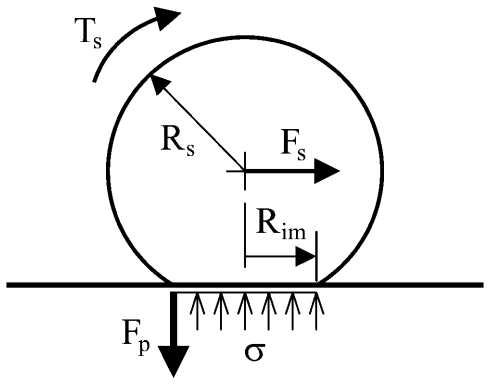

FIGURE 5 Schematic of the force balance on an adherent spherical cell under shear flow. The fluid exerts a drag F_s and a torque T_s on the sphere, creating a moment on the cell that is balanced by the reaction (peeling) force at the trailing edge of the cell F_p and a contact stress σ between the cell and the substrate. The cell radius is R_s and the radius of the contact zone is R_c. The drag and torque on the cell were estimated from the results of Goldman et al. (1967) and the peeling force was obtained by taking a moment balance around the center of the contact zone. The contact stress must balance the vertical reaction force of peeling, F_p, and is assumed to be distributed uniformly over the entire contact area (πR_{im}^2).

1967) to calculate the torque and force on a sphere in contact with a plane wall under shear flow. Dong et al. (1999) has calculated that peeling forces are concentrated in a region that is $<8\%$ of the total contact area. Therefore we treat the peeling force as a point load applied at the trailing edge of the cell, and apply a moment balance at the center of the contact zone. For wall shear stresses of 0.1–1.0 pN/μm^2 (1.0–10 dyn/cm^2) the reaction (peeling) force at the trailing edge of an adherent leukocyte is estimated to be in the range of 100–1500 pN. This vertical component of the peeling stress must be balanced by the reaction (impingement) stress in the remainder of the contact zone. This translates into a contact stress on the order of 5–50 pN/μm^2, depending on what assumptions are made about the size of the contact area over which the stress is distributed. This encompasses the range of contact stresses imposed in the present study where there are clear effects of changing contact stress on adhesion probability.

CONCLUSIONS

Impingement force affects the probability that neutrophils will bond to ICAM-1 presenting surfaces in two ways. When the curvatures of the interacting surfaces are constant, such that the contact stress also remains unchanged, the adhesion probability increases linearly with the area of contact. Additional effects are observed when the contact stress is altered by changing the curvature of the interacting surfaces. In this case, increasing contact stress results in substantial increases in adhesion probability.

The authors thank Richard Bauserman and Donna Brooks for technical support, and Dr. Jean Shaffer for assistance with histologic evaluation of leukocyte populations.

This work was supported by the US Public Health Service under National Institutes of Health grant PO1 HL 18208.

REFERENCES

Alon, R., R. C. Fuhlbrigge, E. B. Finger, and T. A. Springer. 1996. Interactions through L-selectin between leukocytes and adherent leukocytes nucleate rolling adhesions on selectins and VCAM-1 in shear flow. *J. Cell Biol.* 135:849–865.

Alon, R., D. A. Hammer, and T. A. Springer. 1995. Lifetime of the P-selectin-carbohydrate bond and its response to tensile force in hydrodynamic flow. *Nature*. 374:539–542.

Altieri, D. C. 1991. Occupancy of CD11b/CD18 (Mac-1) divalent ion binding site(s) induces leukocyte adhesion. *J. Immunol.* 147:1891–1898.

Bell, G. I. 1978. Models for the specific adhesion of cells to cells. *Science*. 200:618–627.

Bhatia, S., M. King, and D. Hammer. 2003. The state diagram for cell adhesion mediated by two receptors. *Biophys. J.* 84:2671–2690.

Capo, C., F. Garrouste, A. M. Benoliel, P. Bongrand, A. Ryter, and G. I. Bell. 1982. Concanavalin-A-mediated thymocyte agglutination: a model for a quantitative study of cell adhesion. *J. Cell Sci.* 56:21–48.

Chang, K. C., D. F. J. Tees, and D. A. Hammer. 2000. The state diagram for cell adhesion under flow: leukocyte rolling and firm adhesion. *Proc. Natl. Acad. Sci. USA*. 97:11262–11267.

Chesla, S. E., P. Selvaraj, and C. Zhu. 1998. Measuring two-dimensional receptor-ligand binding kinetics by micropipette. *Biophys. J.* 75:1553–1572.

Diamond, M. S., and T. A. Springer. 1993. A subpopulation of Mac-1 (CD11b/CD18) molecules mediates neutrophil adhesion to ICAM-1 and fibrinogen. *J. Cell Biol.* 120:545–556.

Dong, C., J. Cao, E. J. Struble, and H. H. Lipowsky. 1999. Mechanics of leukocyte deformation and adhesion to endothelium in shear flow. *Ann. Biomed. Eng.* 27:298–312.

Dong, C., and X. X. Lei. 2000. Biomechanics of cell rolling: shear flow, cell-surface adhesion, and cell deformability. *J. Biomech.* 33:35–43.

Dransfield, I., C. Cabanas, A. Craig, and N. Hogg. 1992. Divalent cation regulation of the function of the leukocyte integrin LFA-1. *J. Cell Biol.* 116:219–226.

Dustin, M. L., R. Rothlein, A. K. Bhan, C. A. Dinarello, and T. A. Springer. 1986. Induction by IL 1 and interferon-gamma: tissue distribution, biochemistry, and function of a natural adherence molecule (ICAM-1). *J. Immunol.* 137:245–254.

Erlandsen, S. L., S. R. Hasslen, and R. D. Nelson. 1993. Detection and spatial distribution of the β2 integrin (Mac-1) and L-selectin (LECAM-1) adherence receptors on human neutrophils by high-resolution field emission SEM. *J. Histochem. Cytochem.* 41:327–333.

Fernandez-Segura, E., J. M. Garcia, and A. Campos. 1996. Topographic distribution of CD18 integrin on human neutrophils as related to shape changes and movement induced by chemotactic peptide and phorbol esters. *Cell. Immunol.* 171:120–125.

Finger, E. B., K. D. Puri, R. Alon, M. B. Lawrence, U. H. von Andrian, and T. A. Springer. 1996. Adhesion through L-selectin requires a threshold hydrodynamic shear. *Nature*. 379:266–269.

Firrell, J. C., and H. H. Lipowsky. 1989. Leukocyte margination and deformation in mesenteric venules of rat. *Am. J. Physiol.* 256:H1667–H1674.

Goldman, A. J., R. G. Cox, and H. Brenner. 1967. Slow viscous motion of a sphere parallel to a plane wall-II Couette flow. *Chem. Eng. Sci.* 22: 653–660.

Green, C. E., D. N. Pearson, R. T. Camphausen, D. E. Staunton, and S. I. Simon. 2004. Shear-dependent capping of L-selectin and P-selectin glycoprotein ligand 1 by E-selectin signals activation of high-avidity β2-integrin on neutrophils. *J. Immunol.* 172:7780–7790.

Greenberg, A. W., D. K. Brunk, and D. A. Hammer. 2000. Cell-free rolling mediated by L-selectin and sialyl Lewis(x) reveals the shear threshold effect. *Biophys. J.* 79:2391–2402.

Lawrence, M. B., C. W. Smith, S. G. Eskin, and L. V. McIntire. 1990. Effect of venous shear stress on CD18-mediated neutrophil adhesion to cultured endothelium. *Blood.* 75:227–237.

Lawrence, M. B., and T. A. Springer. 1991. Leukocytes roll on a selectin at physiologic flow rates: distinction from and prerequisite for adhesion through integrins. *Cell. Immunol.* 65:859–873.

Lei, X., M. B. Lawrence, and C. Dong. 1999. Influence of cell deformation on leukocyte rolling adhesion in shear flow. *J. Biomech. Eng.* 121:636–643.

Levin, J. D., H. P. Ting-Beall, and R. M. Hochmuth. 2001. Correlating the kinetics of cytokine-induced E-selectin adhesion and expression on endothelial cells. *Biophys. J.* 80:656–667.

Li, R., P. Rieu, D. L. Griffith, D. Scott, and M. A. Arnaout. 1998. Two functional states of the CD11b A-domain: correlations with key features of two Mn^{2+}-complexed crystal structures. *J. Cell Biol.* 143:1523–1534.

Lomakina, E. B., and R. E. Waugh. 2004. Micromechanical tests of adhesion dynamics between neutrophils and immobilized ICAM-1. *Biophys. J.* 86:1223–1233.

Lomakina, E. B., C. M. Spillmann, M. R. King, and R. E. Waugh. 2004. Rheological analysis and measurement of neutrophil indentation. *Biophys. J.* 87:4246–4258.

Rainger, G. E., C. Buckley, D. L. Simmons, and G. B. Nash. 1997. Cross-talk between cell adhesion molecules regulates the migration velocity of neutrophils. *Curr. Biol.* 7:316–325.

Riha, P., D. Dumas, V. Latger, S. Muller, and J. F. Stoltz. 2003. The cooperative effect of L-selectin clusters and velocity-dependent bond formation that stabilizes leukocyte rolling. *Biorheology*. 40:161–166.

Shao, J. Y., and R. M. Hochmuth. 1996. Micropipette suction for measuring picoNewton forces of adhesion and tether formation from neutrophil membranes. *Biophys. J.* 71:2892–2901.

Shao, J. Y., H. P. Ting-Beall, and R. M. Hochmuth. 1998. Static and dynamic lengths of neutrophil microvilli. *Proc. Natl. Acad. Sci. USA*. 95:6797–6802.

Spillmann, C., D. Osorio, and R. E. Waugh. 2002. Integrin activation by divalent ions affects neutrophil homotypic adhesion. *Ann. Biomed. Eng*. 30:1002–1011.

Staunton, D. E., M. L. Dustin, H. P. Erickson, and T. A. Springer. 1990. The arrangement of the immunoglobulin-like domains of ICAM-1 and the binding sites for LFA-1 and rhinovirus. *Cell*. 61:243–254.

Tominaga, Y., Y. Kita, A. Satoh, S. Asai, K. Kato, K. Ishikawa, T. Horiuchi, and T. Takashi. 1998. Affinity and kinetic analysis of the molecular interaction of ICAM-1 and leukocyte function-associated antigen-1. *J. Immunol*. 161:4016–4022.

van Kooyk, Y., and C. G. Figdor. 2000. Avidity regulation of integrins: the driving force in leukocyte adhesion. *Curr. Opin. Cell Biol*. 12:542–547.

Williams, T. E., S. Nagarajan, P. Selvaraj, and C. Zhu. 2001. Quantifying the impact of membrane microtopology on effective two-dimensional affinity. *J. Biol. Chem*. 276:13283–13288.